



Featured article on ECI – Original research paper

Detection of *Bacillus anthracis* spores: comparison of quantum dot and organic dye labeling agents

William C. Schumacher^a, Andrew J. Phipps^b, Prabir K. Dutta^{a,*}

^aDepartment of Chemistry, Ohio State University, 100 West 18th Avenue, Columbus, OH 43210, USA

^bDepartment of Veterinary Biosciences, Ohio State University, USA

ARTICLE INFO

Article history:

Received 5 January 2009

Received in revised form 10 March 2009

Accepted 18 March 2009

Keywords:

Quantum dot

R-Phycoerythrin

Biological labeling

Bacillus anthracis spore

Jurkat T-cell

Flow cytometry

ABSTRACT

Organic dyes are routinely used in labeling assays and sensing of biological molecules. Semiconductor quantum dots (QDs) have attractive features, particularly good resistance to photobleaching and narrow emission bands, which make them potential replacements for organic dyes. Using a previously identified synthetic peptide, a QD, and the R-phycoerythrin (RPE) dye, we have examined various labeling strategies for detecting *Bacillus anthracis* spores. The RPE dye performed well, but we were unable to demonstrate successful binding of the QD by flow cytometry or confocal microscopy. Using a related conjugation strategy, Jurkat T-cells were labeled via a monoclonal antibody (mAb) that binds to the CXCR4 chemokine receptor, CXCR4. It was noted that both QD and RPE labeled the cells. Based on electron microscopy data, we propose that a dense network of fibers on the *Bacillus anthracis* spore surface prevented the QD, but not RPE, from binding. These results suggest that the nature of the biological surface must be considered when using QDs as replacements for organic dyes in biological sensing.

© 2009 The Society of Powder Technology Japan. Published by Elsevier B.V. and The Society of Powder Technology Japan. All rights reserved.

1. Introduction

R-Phycoerythrin (RPE) and fluorescein isothiocyanate (FITC) are traditional labeling agents [1,2], but these and other organic dyes suffer from the following spectral features: (i) wavelength-dependent absorption spectra; (ii) broad and asymmetric emission spectra; and (iii) susceptibility to photobleaching. Such properties reduce the range of usable excitation and detection wavelengths as well as the time period over which labeled targets may be analyzed by techniques like flow cytometry and laser-scanning confocal microscopy [3,4]. Despite these limitations, organic dyes are used routinely in labeling assays because they have high quantum yields and can be conjugated to a variety of target-specific ligands.

An alternative to organic dyes is colloidal QDs which feature optical properties that are dependent on particle size, composition, and the method of production [5,6]. In comparison to most organic dyes, QDs are relatively large (diameter \approx 2–15 nm) and composed of inorganic semiconductors; but spectroscopically, they behave similar to discrete molecules due to quantum confinement. Most colloidal QDs are engineered as core/shell nanoparticles in which a 2–8 nm metalloid core is coated with a thin protective layer of a higher bandgap metalloid shell (e.g., CdSe/ZnS). The shell enhances the QD's emissive properties by confining excited electrons to the core. Provided the density of defect sites at the core/shell

interface is low, QDs can exhibit several advantages over organic dyes, including broad and continuous absorption spectra, narrow and symmetric emission spectra, and resistance to photobleaching. For flow cytometry and confocal microscopy, this translates into longer analysis times and the ability to simultaneously excite and detect multiple fluorophores using a single light source [7–9]. Recently, many surface coating strategies have been developed to provide the QD with solubility in water and reactive groups for conjugation of targeting ligands [10,11]. As such, QDs are increasingly being utilized in biological assays to label a range of targets, including cells, DNA, and recently, pathogenic microorganisms [12–14].

In this paper, we compared the labeling properties of a commercial QD (Qdot[®]) and RPE for detecting *Bacillus anthracis* spores. These methods are promising alternatives to PCR-based assays [15] and mass-based devices [16,17] because they rely only on simple labeling procedures to rapidly detect characteristic antigens on intact spores. The fluorophores were attached to *B. anthracis* spores by using one or more of the following conjugation strategies: (i) one-step sulfo-SMCC conjugate assay; (ii) two-step streptavidin–biotin assay; (iii) one-step streptavidin–biotin conjugate assay; and (iv) one-step PEG₇₅₀₀ conjugate assay. We also confirmed the viability of our conjugation methods by using a Jurkat T-cell assay in which the fluorophores were attached via a two-step streptavidin–biotin strategy. The performance (i.e., brightness) of fluorescently-labeled targets was qualified by confocal microscopy and quantified by flow cytometry. These results establish a new set

* Corresponding author. Tel.: +1 614 292 4532; fax: +1 614 688 5402.

E-mail address: dutta@chemistry.ohio-state.edu (P.K. Dutta).

of experimental boundaries for the still-developing field of Qdot biological sensing.

2. Materials and methods

2.1. *B. anthracis* spores and Jurkat T-Cells

B. anthracis Sterne spores (seed from the live spore veterinary vaccine, Colorado Serum Company) were grown, isolated, and purified according to previously established methods [18–21]. Jurkat T-cells (clone E6-1; American Type Culture Collection) were maintained in RPMI 1640 supplemented with 10% fetal bovine serum, penicillin (100 µg/mL), streptomycin (100 µg/mL), and L-glutamine (0.03 mg/mL).

2.2. *B. anthracis* spore labeling

2.2.1. One-step sulfo-SMCC conjugate assay

A *B. anthracis* spore-specific peptide, ATYPLPIRGGG (ATYP, GenScript Corporation), was conjugated to RPE (Invitrogen) or Qdot585 ITK amino-PEG quantum dot (Qdot585, Invitrogen) through the heterobifunctional crosslinker sulfo-succinimidyl-4-(*N*-maleimidomethyl)cyclohexane-1-carboxylate (sulfo-SMCC, Pierce) according to previously described methods [22,23]. Spores (10^6) were rinsed in staining buffer (calcium/magnesium-free PBS buffer, 1% fetal bovine serum, pH 7.2), then mixed with either 2 µM ATYP-RPE or 1 µM ATYP-Qdot585 and incubated for 1 h at 37 °C. Unbound conjugate was removed by rinsing the spores three times with 200 µL volumes of wash buffer (1× PBS, pH 7.4). Centrifugation (700g at 4 °C for 5 min) was used to collect spores in between each wash step. Labeled spores were analyzed immediately following chemical fixation by 2% paraformaldehyde (PFA). To evaluate nonspecific binding, spores were incubated with either 2 µM RPE or 1 µM Qdot585 (no ATYP peptide) and processed similarly.

2.2.2. Two-step streptavidin–biotin assay

Spores (10^6) were rinsed in staining buffer then mixed with 3 mg/mL of a biotinylated version of the ATYP peptide, ATYPLPIRGGG{K-biotin} (ATYP-bio, GenScript Corporation), and incubated for 1 h at 37 °C. Unbound peptide was removed by repeated wash/centrifuge steps. Bound peptide was detected by incubating with either 50 µg/mL streptavidin-RPE (SA-RPE, Invitrogen) or 100 nM streptavidin-Qdot585 (SA-Qdot585, Invitrogen) for an additional hour at 37 °C. After removing unbound labeling agent, the samples were fixed in 2% PFA and analyzed. As a control, unlabeled spores (no ATYP-bio peptide) were incubated with either 50 µg/mL SA-RPE or 100 nM SA-Qdot585 and processed similarly. SA-Qdot565 was also used for this assay.

2.2.3. One-step streptavidin–biotin conjugate assay

We modified the previous streptavidin–biotin assay by conjugating the ATYP-bio peptide to SA-Qdot585 before incubation with *B. anthracis* spores [24]. Unlabeled spores (10^6) were rinsed in staining buffer then incubated for 1 h at 37 °C with 100 nM of the dialysis-purified conjugate. Repeated wash/centrifuge steps were used to remove unbound conjugate. Labeled samples were fixed in 2% PFA and immediately analyzed. As a control, spores were incubated with 100 nM SA-Qdot585 (no ATYP-bio peptide) and processed similarly.

2.2.4. One-step PEG₇₅₀₀ conjugate assay

The ATYP peptide was also conjugated to Qdot585 via the heterobifunctional crosslinker maleimide–PEG₇₅₀₀–NHS ester (PEG₇₅₀₀, JenKem Technology CO., LTD). The conjugation reaction was performed according to the same procedure used for sulfo-SMCC

conjugation. Spores (10^6) were rinsed in staining buffer then mixed with 100 nM ATYP-Qdot585 and incubated for 1 h at 37 °C. Unbound conjugate was removed by repeated wash/centrifuge steps, and labeled spores were analyzed immediately following chemical fixation by 2% PFA. As a control, spores were incubated with 100 nM Qdot585 (no ATYP peptide) and processed similarly.

2.3. T-cell labeling

2.3.1. Two-step streptavidin–biotin assay

T-cells (10^6) were rinsed in staining buffer then mixed with 10 µg/mL of a biotinylated mAb against the human CXCR4 receptor (CXCR4-bio, R&D Systems, Inc.) and incubated for 1 h at 37 °C. Unbound mAb was removed by repeated wash/centrifuge steps. Bound mAb was detected by incubating with either 2 µg/mL SA-RPE or 20 nM SA-Qdot585 for an additional hour at 37 °C. Following the removal of unbound labeling agent, samples were fixed in 2% PFA and immediately analyzed. To evaluate nonspecific binding of the labeling agents, unlabeled cells (no CXCR4-bio mAb) were incubated with either 2 µg/mL SA-RPE or 20 nM SA-Qdot585 and processed similarly.

2.4. Characterization techniques

2.4.1. Flow cytometry

Labeled targets were analyzed using a FACSCalibur instrument and CellQuest Pro software (Becton Dickinson Biosciences). All samples were excited at 488 nm with an argon-ion laser and detected using the FL2 (PE; 585 ± 21 nm) bandpass filter. Unlabeled spores/cells and nonspecific binding controls were used to empirically determine the voltage and gain for positively-labeled samples. Representative FL2 voltage/gain values were 543 and 1.00, respectively. The compensation was set to zero for all samples. Mean channel fluorescence (MCF) values were recorded for negatively labeled and positively labeled populations. All flow cytometry histograms were presented as an average of 10,000 events.

2.4.2. Confocal microscopy

Samples were analyzed using a Leica TCS SP2 AOBs confocal laser scanning microscope. A 10 µL aliquot of labeled spores was deposited on a clean glass microscope slide and gently heated at 30 °C to immobilize the spores. Dried spores were mounted with 90% glycerol, then cover-slipped and imaged immediately. Cells were deposited on poly-L-lysine treated microscope slides, mounted in 50% glycerol, and imaged thereafter. All samples were excited at 488 nm with an argon-ion laser and detected using FL2 (575 ± 30 nm). Unlabeled spores/cells and nonspecific binding controls were used to empirically determine the FL2 voltage for positive samples, which was typically 600. All images were collected using a 40× oil objective lens and presented as an average of ten scans. Confocal $xy\lambda$ scans, which measured the fluorescence intensity across a range of wavelengths, were also performed to confirm the source of emission.

2.4.3. Transmission electron microscopy

Unlabeled spores or cells were pre-fixed with 5% glutaraldehyde in 20 mM sodium phosphate buffer, pH 7.2 for three days at room temperature. Post-fixation was carried out with 1% osmium tetroxide in 50 mM sodium phosphate buffer, pH 7.2 for 24 h at room temperature. Serial alcohol dehydration was then performed using ethanol (15, 35, 50, 75, 90, and 100% × 3) and then acetone (100% × 3). Next the samples were embedded with epon resin and polymerized at 75 °C for 24 h. Ultra-thin sections were obtained using an LKB Ultramicrotome (Sweden). The sections were double-stained with 1% uranyl acetate and lead citrate. EM observation was made by a Phillips EM 300 transmission electron micro-

scope at an accelerating voltage of 60 kV. The images were recorded on Kodak electron image films.

HRTEM images of the Qdots were obtained by using a Tecnai-F20 system with an acceleration voltage of 200 kV. The Qdots were deposited from a dilute solution onto a non-Formvar copper grid with an ultra-thin carbon film on a holey carbon support film.

3. Results

3.1. Labeling agents

Fig. 1a shows the HRTEM of the Qdot 585 used in this study. From the electron micrograph, we estimated the core/shell nanoparticle to be 5–6 nm in diameter. However, the overall size of the Qdot is not solely determined by the CdSe/ZnS, as it is also coated with a carboxylated polymer and functionalized with long chain PEG units. These outer layers, which are not electron-dense enough to be imaged by TEM, extend the overall diameter to approximately 12–15 nm. The molecular weight of the Qdot is around 1–2 MDa. SA-Qdot585 contained 5–10 SA proteins per Qdot585. RPE is a globular protein belonging to the phycobiliprotein family of fluorescent dyes. It has approximate dimensions of 12 nm × 12 nm × 6 nm based on X-ray crystallography data [25] and a molecular weight of 240 kDa. SA-RPE contained 1–3 SA proteins per RPE. Fig. 1b and c shows the HRTEM images of the *B. anthracis* spores that were examined in this study. Two types of spores were distinguished, with (Fig. 1b) and without (Fig. 1c) the exosporium.

3.2. *B. anthracis* spore labeling

Schematic illustrations for each of the *B. anthracis* spore conjugation strategies are shown in Fig. 2.

3.2.1. One-step sulfo-SMCC conjugate assay (Fig. 2a)

The ATYP peptide was conjugated to RPE and Qdot585 via the sulfo-SMCC crosslinker. *B. anthracis* spores were then incubated with either the ATYP-RPE or ATYP-Qdot585 conjugate and analyzed by flow cytometry (Fig. 3). Unlabeled *B. anthracis* spores had intrinsic fluorescence, as indicated by a histogram pattern centered near the first decade of fluorescence shown in Fig. 4a. However, instrumental settings on the flow cytometer were adjusted so that only 0.01% of these spores were recognized as positive events. We also evaluated nonspecific binding by incubating the labeling agents (no ATYP peptide) with unlabeled spores, but neither RPE (Fig. 4b, 0.46% positive) nor Qdot585 (Fig. 4c, 0.14% positive) were found to significantly stain the spore surface. After treatment with ATYP-RPE, 73% of the spores were detected as positive events by flow cytometry (Fig. 3a). Conversely, only 0.52% of ATYP-Qdot585 treated spores were detected as positive events (Fig. 3b). Confocal microscopy analysis showed heavy spore-bound fluorescence in

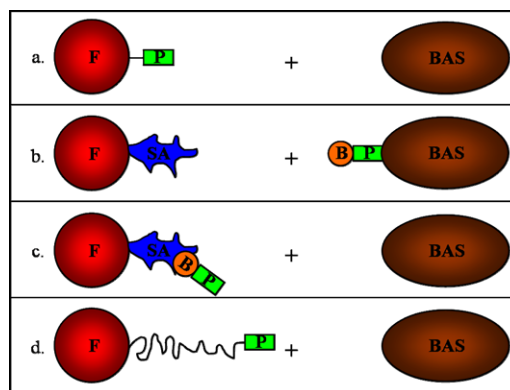


Fig. 2. Schematic illustrations of the *B. anthracis* spore conjugation strategies used here. (a) One-step sulfo-SMCC conjugate assay; (b) two-step streptavidin-biotin assay; (c) one-step streptavidin-biotin conjugate assay; and (d) one-step PEG₇₅₀₀ conjugate assay. F, fluorophore; P, ATYP peptide; SA, streptavidin; B, biotin, BAS, *Bacillus anthracis* spore.

the case of ATYP-RPE (Fig. 3a) and only trace fluorescence from spores incubated with ATYP-Qdot585 (Fig. 3b). Additionally, $\chi\lambda$ scans confirmed that RPE was the source of emission on ATYP-RPE-labeled spores (Fig. 3a), and spore autofluorescence was responsible for the measured emission on spores incubated with ATYP-Qdot585 (Fig. 3b) (as evidenced from the inset of Fig. 3).

3.2.2. Two-step streptavidin-biotin assay (Fig. 2b)

B. anthracis spores were incubated with the ATYP-bio peptide. In a separate step, bound peptide was detected using either the SA-RPE or SA-Qdot585 labeling agent. Fig. 5 (and Fig. 6) shows representative flow cytometric data for this assay. Compared to unlabeled *B. anthracis* spores (Fig. 6a, 0.24% positive), both SA-RPE (Fig. 6b, 1.8% positive) and SA-Qdot585 (Fig. 6c, 3.7% positive) non-specifically stained the spore surface. Although the histogram patterns for the nonspecific controls did not noticeably shift, the non-zero baselines beyond the first decade of fluorescence accounted for the increased brightness. Following treatment with the ATYP-bio peptide, 53% of *B. anthracis* Sterne spores were positively detected by SA-RPE (Fig. 5a) as opposed to only 4.6% by SA-Qdot585 (Fig. 5b).

3.2.3. One-step streptavidin-biotin conjugate assay (Fig. 2c)

We modified the previous two-step streptavidin-biotin assay by conjugating SA-Qdot585 to the ATYP-bio peptide beforehand. *B. anthracis* spores were then incubated with the ATYP-bio-SA-Qdot585 conjugate and analyzed by flow cytometry (Fig. 7). Unlabeled spores fluoresced, but only 0.23% were registered as positive events by the flow cytometer (Fig. 7a). Although 4.2% of ATYP-bio-SA-Qdot585 treated spores were positively labeled (Fig. 7c), this

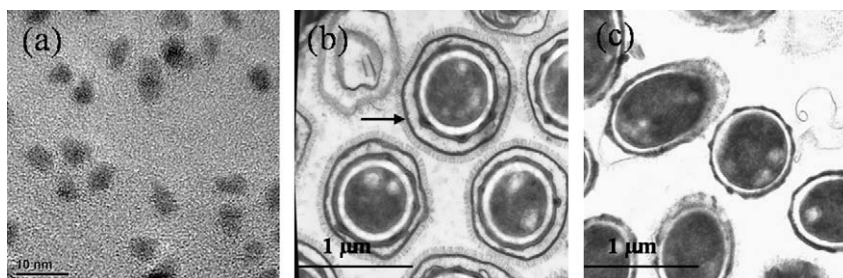


Fig. 1. (a) HRTEM of Qdot585 used in this study. The CdSe/ZnS portion of the Qdot is approximately ellipsoidal. Outer organic layers of the Qdot are not visible by TEM. TEM of (b) a population of *B. anthracis* spores which possessed an intact exosporium (arrow), and (c) a population of *B. anthracis* spores which lacked an outer exosporium.

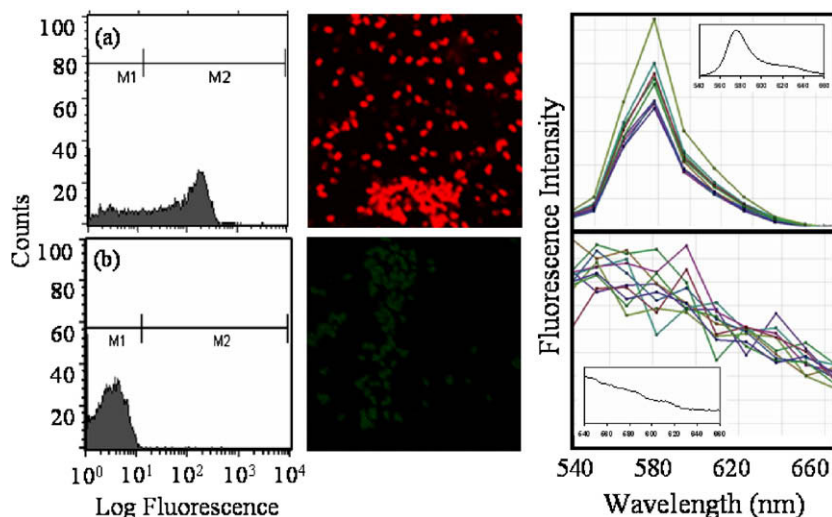


Fig. 3. Flow cytometric histograms and confocal images for the one-step (a) ATYP-RPE and (b) ATYP-Qdot585 sulfo-SMCC conjugate spore assays. Flow cytometric statistical data is as follows: ATYP-RPE conjugate, 73% positive with MCF = 128; ATYP-Qdot585 conjugate, 0.52% positive with MCF = 96. Confocal $xy\lambda$ scans showing that the fluorescence measured from confocal images was due to (a) RPE or (b) spore autofluorescence. Ten randomly selected spores were used for each $xy\lambda$ analysis. For comparison, the solution fluorescence spectra for (a) RPE and (b) *B. anthracis* Sterne spores are presented in the insets.

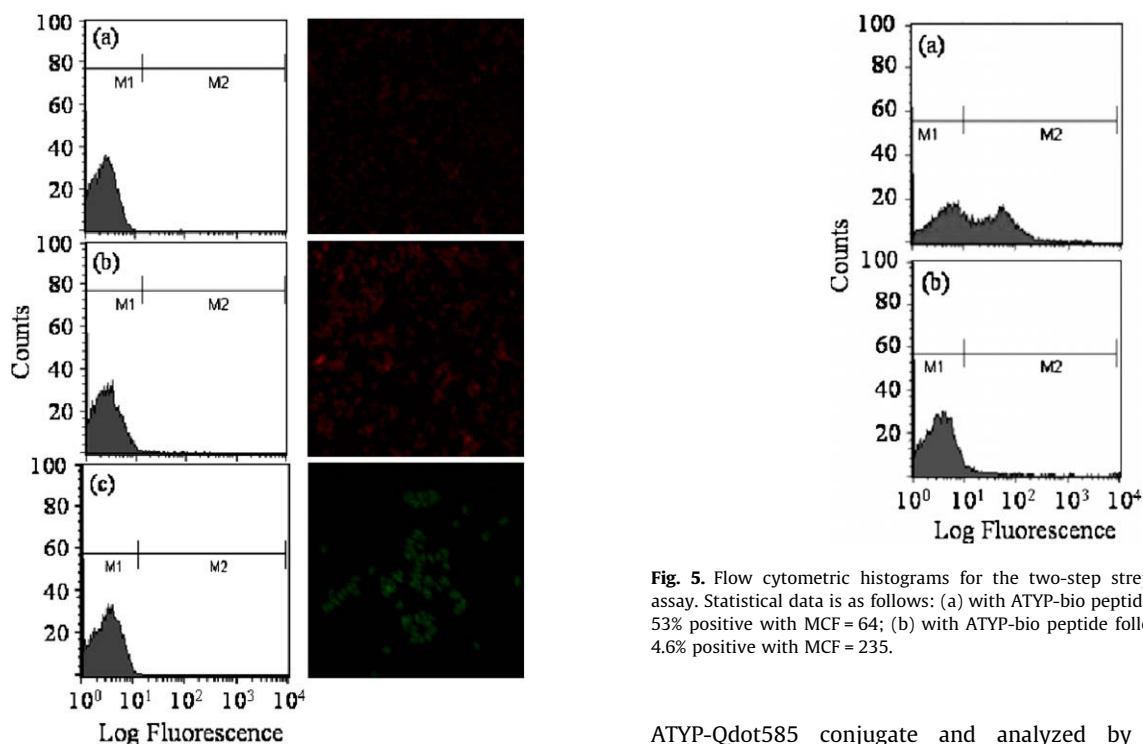


Fig. 4. Control histograms and confocal images one-step sulfo-SMCC conjugate spore assays. Flow cytometric statistical data is as follows: (a) unlabeled spores, 0.01% positive with MCF = 20; (b) with RPE, 0.46% positive with MCF = 51; (c) with Qdot585) 0.14% positive with MCF = 92.

value was only incrementally higher than the percentage of spores nonspecifically stained by SA-Qdot585 (Fig. 7b, 2.6% positive).

3.2.4. One-step PEG₇₅₀₀ conjugate assay (Fig. 2d)

We conjugated Qdot585 to the ATYP peptide through a heterobifunctional PEG crosslinker, designed to provide greater spatial distance between the fluorophore and the spore. PEG₇₅₀₀ possessed the same reactivity as sulfo-SMCC but was significantly longer (≈ 50 nm long). *B. anthracis* spores were incubated with the

Fig. 5. Flow cytometric histograms for the two-step streptavidin–biotin spore assay. Statistical data is as follows: (a) with ATYP-bio peptide followed by SA-RPE, 53% positive with MCF = 64; (b) with ATYP-bio peptide followed by SA-Qdot585, 4.6% positive with MCF = 235.

ATYP-Qdot585 conjugate and analyzed by flow cytometry (Fig. 8). Unlabeled spores (Fig. 8a, 0.16% positive) and the Qdot585 nonspecific binding control (Fig. 8b, 0.54% positive) behaved as expected, but this conjugate, too, was unable to detect *B. anthracis* spores (Fig. 8c, 1.26% positive).

All of the *B. anthracis* spores used in the studies described above were characterized by the HRTEM shown in Fig. 1b. In testing different lots of *B. anthracis* spores with these assays, we found one lot that occasionally resulted in positive Qdot labeling. Using the two-step streptavidin–biotin assay, we detected SA-Qdot565 on the surface of some populations of *B. anthracis* spores that had been incubated with the ATYP-bio peptide (Fig. 9a). Alternatively, SA-Qdot565 did not bind to spores that were not incubated with the ATYP-bio peptide (Fig. 9b). The HRTEM of spores that were detectable by Qdots was characterized by the electron micrographs in Fig. 1c, and did not possess an outermost exosporium. We attrib-

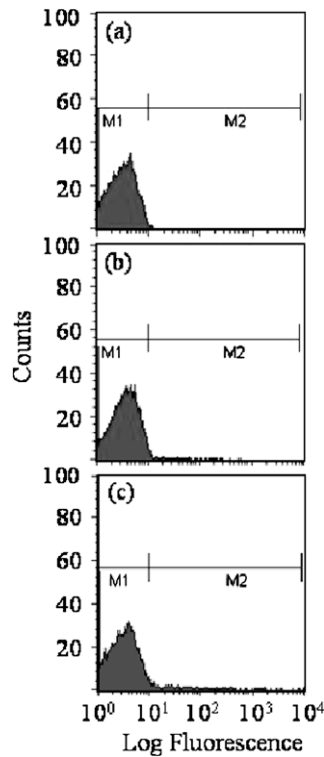


Fig. 6. Control histograms of a two-step streptavidin–biotin spore assay. Flow cytometric statistical data is as follows: (a) unlabeled spores, 0.24% positive with MCF = 11; (b) with SA-RPE, 1.8% positive with MCF = 50; (c) with SA-Qdot585, 3.7% positive with MCF = 304.

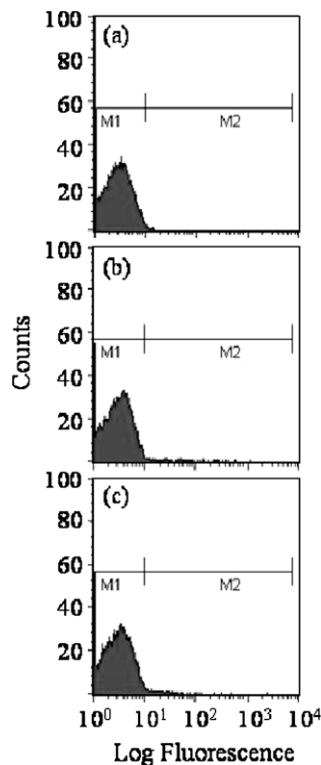


Fig. 7. Flow cytometric data for the one-step streptavidin–biotin conjugate spore assay. Statistical data is as follows: (a) unlabeled spores, 0.23% positive with MCF = 12; (b) with SA-Qdot585, 2.6% positive with MCF = 198; (c) with ATYP-bio-SA-Qdot585 conjugate, 4.2% positive with MCF = 242.

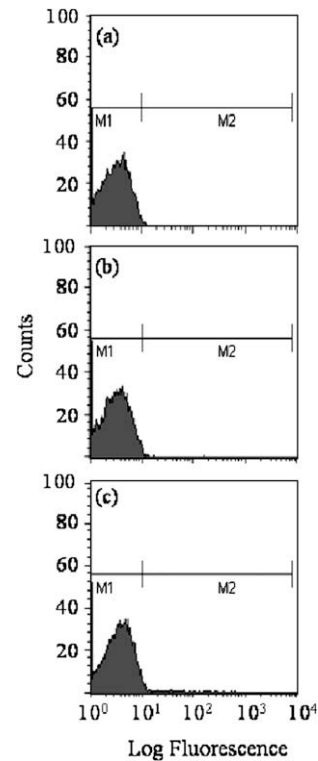


Fig. 8. Flow cytometric data for the one-step ATYP-Qdot585 PEG₇₅₀₀ conjugate spore assay. Statistical data is as follows: (a) unlabeled spores, 0.16% positive with MCF = 14; (b) with Qdot585, 0.54% positive with MCF = 146; (c) with ATYP-Qdot585 conjugate, 1.26% positive with MCF = 251.

uted the absence of the exosporium to repeated handling during the prolonged storage period (4 years) of this particular lot or unknown protease activity, possibly through contamination.

3.3. T-cell Labeling

3.3.1. Two-step streptavidin–biotin assay

T-cells were treated with a biotinylated mAb that binds to the CXCR4 receptor. We chose to detect this receptor because it is a highly expressed protein on the surface of Jurkat T-cells [26], and thus, a good candidate for evaluating the performance of our labeling agents. The CD4 receptor on T-cells has also been utilized similarly [27]. T-cell-bound mAb was detected using either SA-RPE or SA-Qdot585. Figs. 10 and 11 show typical flow cytometry and confocal microscopy data generated by this assay. Unlabeled cells (Fig. 11a, 0.01% positive,) possessed an inherent level of autofluorescence from which the cutoff value for positive events was established. Neither the SA-RPE (Fig. 11b, 0.02% positive) nor SA-Qdot585 (Fig. 11c, 0.12% positive) nonspecific controls stained the surface of unlabeled (no CXCR4-bio mAb) cells. Following treatment with the CXCR4-bio mAb, cells were easily detected by the SA-RPE (Fig. 10a, 100% positive) and SA-Qdot585 (Fig. 10b, 100% positive) labeling agents. However, upon comparing the relative positions of their histogram patterns, it was clear that RPE-labeled cells were brighter than Qdot585-labeled cells (fivefold brighter by MCF values listed in Fig. 10). Incubating mAb-treated cells with higher concentrations of SA-Qdot585 did not increase the brightness measured by the flow cytometer (data not shown). As presented in Fig. 10, confocal microscopy analysis of labeled cells showed that the fluorescence was cell-bound, and $xy\lambda$ scans qualitatively confirmed the measured emission was due to the labeling agents and not autofluorescence.

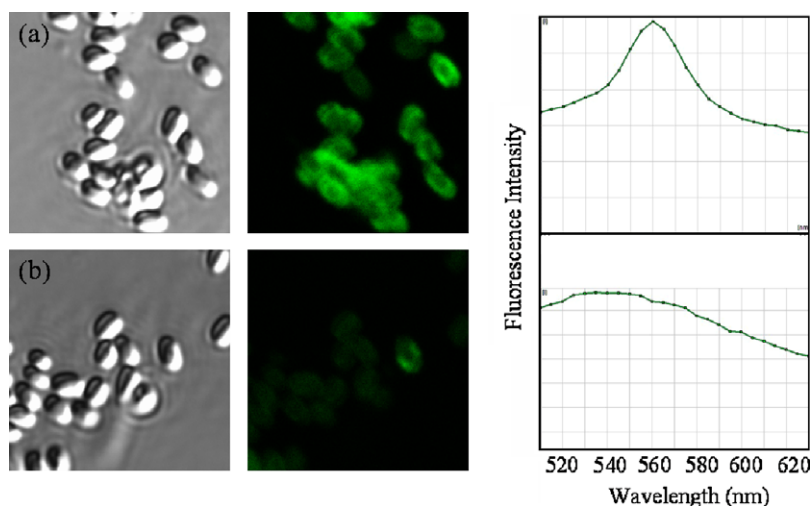


Fig. 9. Confocal images and $xy\lambda$ scans for the two-step streptavidin–biotin assay using SA-Qdot565. Unlike previous attempts, these (a) ATYP-bio peptide-treated *B. anthracis* spores were detected by SA-Qdot565. (b) Spores that were not incubated with the ATYP-bio peptide were not labeled by SA-Qdot565. Confocal $xy\lambda$ scans confirmed the source of fluorescence was (a) Qdot565 or (b) spore autofluorescence.

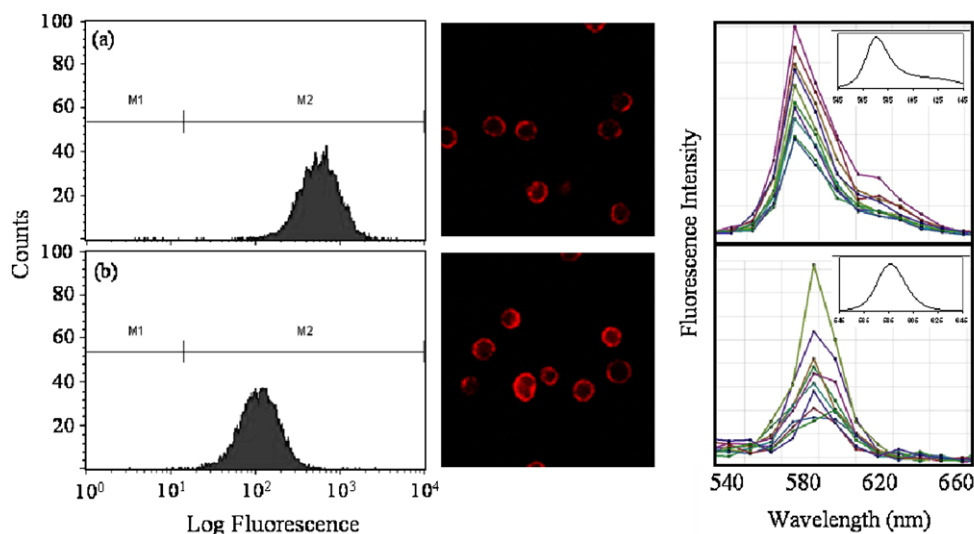


Fig. 10. Representative flow cytometric histograms and confocal images for the two-step streptavidin–biotin T-cell assay. Statistical data determined by flow cytometry is as follows: (a) with CXCR4-bio mAb followed by SA-RPE, 100% positive with MCF = 600; (b), with CXCR4-bio mAb followed by SA-Qdot585, 100% positive with MCF = 120. Confocal $xy\lambda$ scans showing that the fluorescence measured from confocal images was due to (a) SA-RPE or (b) SA-Qdot585. Ten randomly selected cells were used for each $xy\lambda$ analysis. For comparison, the solution fluorescence spectra for (a) SA-RPE and (b) SA-Qdot585 are presented in the insets.

Fluorescently-labeled cells were also measured by flow cytometry as a function of storage time in PBS buffer at 4 °C (Fig. 12). After 2 h of storage, SA-Qdot585-labeled cells lost about 43% of their brightness according to MCF values (Fig. 12c and d). Consequently, almost 35% of the Qdot-labeled cells were registered as negative events by the cytometer even though they were positively labeled. SA-RPE-labeled cells lost approximately 7% of their brightness over the same time period (stored in PBS buffer at 4 °C), but 100% were still detected as positive events (Fig. 12a and b).

4. Discussion

4.1. *B. anthracis* spore labeling

All of these assays utilized a short peptide fragment that was previously shown to bind to the exosporium basal layer of *B. anthracis* spores with good sensitivity and selectivity [23,28]. By

modifying its carboxy terminus to possess different reactive groups, we conjugated the peptide to RPE and the Qdot in a variety of ways designed to identify physical parameters that resulted in successful binding. Various conjugation schemes that altered the distance between the spore and the chromophore were examined. Compared to the one-step sulfo-SMCC conjugate assay (Fig. 2a), the two-step streptavidin–biotin assay (Fig. 2b) resulted in an increased distance between the spore surface and fluorophore. This was similarly the case with the one-step streptavidin–biotin assay (Fig. 2c), except that this modification also limited the number of peptides available for binding to spores because of the finite number of SA proteins on the fluorophores. The final conjugation strategy (Fig. 2d) used PEG₇₅₀₀ to impart even more length and flexibility to the labeling agent. However, when analyzed by flow cytometry and confocal microscopy, only RPE-based assays were consistently successful at labeling the spores (Figs. 3 and 5). Except for certain populations of spores that lacked an exosporium (Fig. 9),

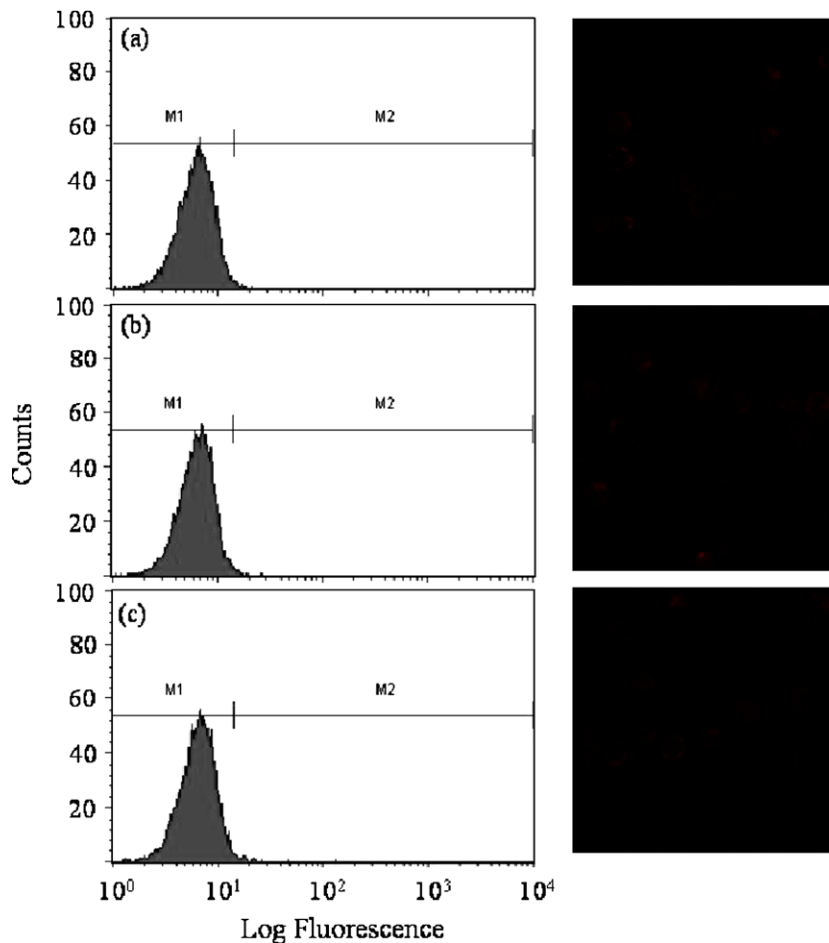


Fig. 11. Control histograms and confocal images for the two-step streptavidin–biotin T-cell assay. Statistical data determined by flow cytometry is as follows: (a) unlabeled T-cells, 0.01% positive with MCF = 14; (b) with SA-RPE, 0.02% positive with MCF = 26; (c) with SA-Qdot585, 0.12% positive with MCF = 34.

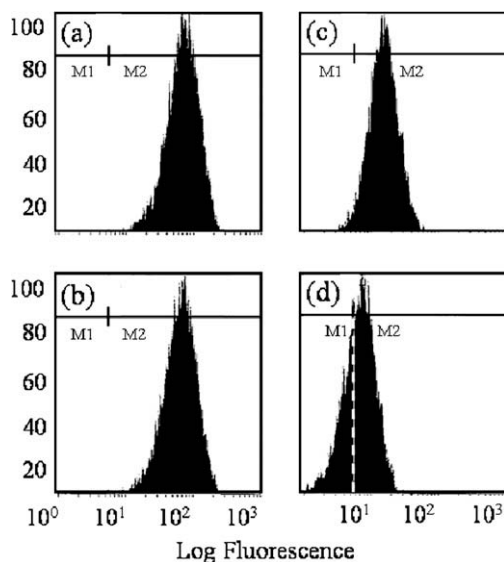


Fig. 12. Flow cytometry histograms for SA-RPE- and SA-Qdot585-labeled T-cells measured immediately after the assay (a, c) or following 2 h of storage in PBS buffer at 4 °C (b, d). Statistical data is as follows: (a) with CXCR4-bio mAb followed by SA-RPE, 100% positive with MCF = 80; (b) with CXCR4-bio mAb followed by SA-RPE, 100% positive with MCF = 76; (c) with CXCR4 -bio mAb followed by SA-Qdot585, 96% positive with MCF = 18; (d) with CXCR4 -bio mAb followed by SA-Qdot585, 60% positive with MCF = 10.

none of the Qdot585-based assays resulted in appreciable spore-bound fluorescence (Figs. 3, 5, 7 and 8). These results were unexpected, as Qdot585 was carefully selected to excite and emit at the same wavelengths and have the same surface chemistry as RPE.

There is only one other example in literature which used Qdots to label *B. anthracis* spores [24]. Using an amino terminus biotinylated version of the ATYP peptide and SA-Qdot585, they formed a one-step conjugate and claimed to detect *B. anthracis* spores with good specificity as compared *Bacillus cereus* and *Bacillus thuringiensis* control strains. However, the flow cytometry data was only indicative of weak binding. In repeating their assay, we decided not to biotinylate the amino terminus of the ATYP peptide for fear that doing so would bury part of the spore-specific region of the peptide (ATYPLP) in the streptavidin protein, which would probably lower the affinity of the conjugate for *B. anthracis* spores. Even though flow cytometry data indicated our conjugate was unsuccessful at detecting *B. anthracis* spores (Fig. 7), we periodically measured fluorescent signals from Qdot585-labeled *B. anthracis* spores by using confocal microscopy. However, after performing $xy\lambda$ scans the signals were always attributed to spore autofluorescence (Figs. 3 and 9). Fig. 13 clearly demonstrates that by simply focusing on z-planes above or below the spores, spore autofluorescence could be observed and altered. This spore autofluorescence is sufficiently intense that it has even been used as a sorting criterion for flow cytometry since most airborne particulates do not have intrinsic fluorescence [29]. After consideration of our data, we feel that the incremental shifts in fluorescence shown by Park et al.

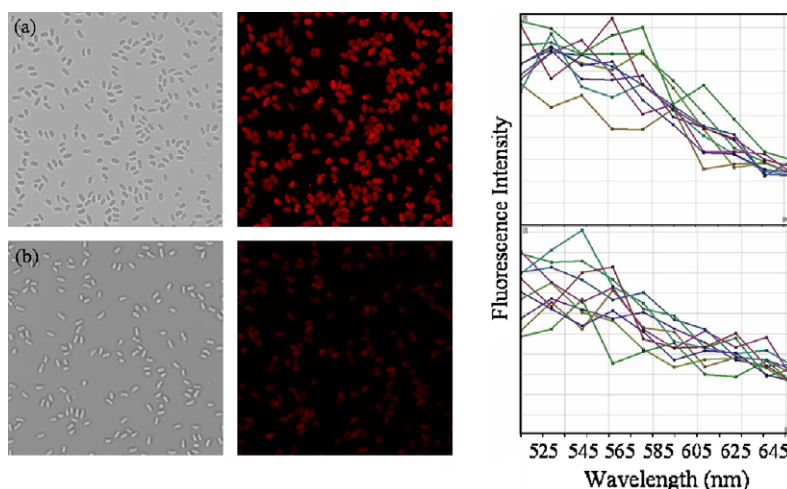


Fig. 13. Confocal images showing that the intensity of spore autofluorescence can be increased or decreased simply by focusing on z-planes (a) above or (b) below spores. Without performing $xy\lambda$ scans, this fluorescence could be mistaken for a spore-bound fluorophore emitting in the specified wavelength region.

could have been caused by spore autofluorescence or nonspecific binding of the Qdot labeling agents [24].

We used the data collected with Jurkat T-cells as a way to confirm that our two-step streptavidin–biotin Qdot labeling strategy worked. One hundred percent of the CXCR4–bio mAb-treated cells were labeled by SA–Qdot585 (Fig. 10). However, SA–Qdot585-labeled cells gradually lost their brightness from temporary storage in PBS buffer (Fig. 12). This behavior was reported previously by Ness et al., who went on to speculate the signal decay was caused by reduced stability of the Qdots in a dilute aqueous environment [30]. Such a signal loss can also be problematic for flow cytometry, as samples are typically stored in buffer and presented to the instrument in suspension. Also, compared to SA–RPE, the lower extinction coefficient of SA–Qdot585 at 488 nm excitation contributed to its weaker fluorescent signal when conjugated to T-cells.

4.2. Surface interactions of *B. anthracis* spores with labeling agents

As seen in Fig. 1b, *B. anthracis* spores normally possess a dense network of surface fibers that are approximately 60 nm-long and composed of a single glycoprotein called the BclA (*Bacillus collagen-like protein of anthracis*) [31,32]. The BclA nap is the primary contact point for the spore and is even dense enough to block some spore-specific antibodies, peptides, and other molecules from binding to their receptors on the exosporium basal layer [33,34].

In this study, only RPE-based labeling agents were routinely detected on the spore surface. While Qdot585 possessed the same optical properties and surface functional groups as RPE, steric and/or electrostatic differences could have reduced its ability to bind to spores. Our hypothesis is that the large size and surface charge of Qdot585 made it unable to diffuse through the BclA fibers and bind. In addition, we speculate that the highly-functionalized Qdot585 may have been repelled electrostatically by the hydrophobic BclA fibers [34]. Gel electrophoresis experiments conducted in our laboratory indicated that Qdot585 carried an overall negative charge (data not shown). We reasoned that by increasing the distance between the spore surface and the Qdot via use of the streptavidin–biotin molecule and the PEG (Fig. 2), we might mitigate any problems caused by surface chemistry or steric hindrance; however, no improvements were observed. Nonetheless, in support of our overall hypothesis are the confocal images shown in Fig. 9 demonstrating that SA–Qdot565 labeled bound ATYP–bio peptide on the surface of a population of *B. anthracis* spores which lacked the outermost exosporium. Boydston et al. identified a sub-

BclA “sac” layer that covered *B. anthracis* spores and was detectable by ATYP–RPE in the absence of the exosporium. While this layer was shown to be fragile when not enclosed by an exosporium, it could be that the sac on SA–Qdot565-labeled spores was still intact [28]. In a previous study by flow cytometry, we have reported that a fraction of these spores will bind the ATYP–RPE conjugate ($\approx 12\%$) [35]. Our data could also indicate that the ATYP peptide binds to other receptors that are located on the multi-protein spore coat.

Of relevance to our current study is an investigation by Ferrari and Bergquist on the interaction of Qdot and organic dye labeling agents with *Cryptosporidium parvum* oocysts [36]. Oocysts and *B. anthracis* spores are similar in appearance and composition [37]. Ferrari and Bergquist observed the brightness of Qdot-labeled oocysts to be significantly lower than organic dye-labeled oocysts. Comparison of the Qdot585 and RPE conjugates revealed that RPE labeling was 13-fold brighter [36]. As a possible explanation, the authors cited a study by Dwarakanath et al., which claimed the fluorescence from QD conjugates was blue-shifted by 60–140 nm following conjugation to bacteria [38]. However, Ferrari and Bergquist did not observe such shifts in their data. The reduced brightness could have arisen from repulsive interactions between the Qdot and oocyst surface, as is being proposed here for *B. anthracis* spores.

5. Conclusions

This study focuses on using quantum dots for detection of *B. anthracis* spores. Using a peptide that has been shown to bind to *B. anthracis* spores, we tested several different conjugation strategies with a Qdot and RPE. We found that most spores could only be detected by using RPE, even after we increased the spacer length between the fluorophore and spore surface. The only exception to this was a spore preparation that lacked the exosporium. We propose the dense network of BclA fibers prevented the Qdot, but not RPE, from binding to the basal layer of the exosporium of *B. anthracis* spores. For Jurkat T-cells, which have no BclA-like fibers, we successfully demonstrated that either fluorophore could be used for detection. Also, we note that additional handling measures must be taken to prevent significant losses in Qdot fluorescence. This study suggests that in developing detection strategies for biological targets, electrostatic and steric interactions between the target surface and the detection probe can play an important role. This is an issue that has not been addressed for detection of most biological targets, including *B. anthracis* spores.

Acknowledgements

This work was supported in part by the National Science Foundation under Grant No. 0221678. We are grateful to Dr. Mamoru Yamaguchi and Hendrick Colijn for performing the electron microscopy work.

References

- [1] A. Glazer, Phycobiliproteins – a family of valuable widely used fluorophores, *Journal of Applied Phycology* 6 (1994) 105–112.
- [2] M. Mullins, Overview of fluorochromes, in: L. Javois (Ed.), *Methods in Molecular Biology*, vol. 115, Humana Press, New York, 1999, pp. 97–105.
- [3] S. Paddock, Practices and principles of laser scanning confocal microscopy, *Molecular Biotechnology* 16 (2000) 127–149.
- [4] W. Parak, T. Pellegrino, C. Plank, Labeling of cells with quantum dots, *Nanotechnology* 16 (2005) R9–R25.
- [5] P. Alivisatos, Semiconductor clusters, nanocrystals, and quantum dots, *Science* 271 (1996) 933–937.
- [6] A. Yoffe, Semiconductor quantum dots and related systems: electronic, optical, luminescence, and related properties of low-dimensional systems, *Advances in Physics* 50 (2001) 1–208.
- [7] M. Seydack, Nanoparticle labels in immunosensing using optical detection methods, *Biosensors and Bioelectronics* 20 (2005) 2454–2469.
- [8] I. Medintz, H. Uyeda, E. Goldman, H. Mattoussi, Quantum dot bioconjugates for imaging, labeling, and sensing, *Nature Materials* 4 (2005) 435–446.
- [9] P. Cattopadhyay, J. Yu, M. Roederer, Application of quantum dots to multicolor flow cytometry, in: MC. Hotz, M. Bruchez (Eds.), *Methods in Molecular Biology*, vol. 374, Humana Press, New York, 2007, pp. 175–184.
- [10] H. Mattoussi, M. Mauro, E. Goldman, G. Anderson, V. Sundar, F. Mikulec, M. Bawendi, Self-assembly of CdSe–ZnS quantum dot bioconjugates using an engineered recombinant protein, *Journal of the American Chemical Society* 122 (2000) 12142–12150.
- [11] W. Yang, E. Chang, J. Falkner, J. Zhang, A. Al-Somali, C. Sayes, J. Johns, R. Drezek, V. Colvin, Forming biocompatible and nonaggregated nanocrystals in water using amphiphilic polymers, *Journal of the American Chemical Society* 129 (2007) 2871–2879.
- [12] M. Bruchez, M. Moronne, P. Gin, S. Weiss, P. Alivisatos, Semiconductor nanocrystals as fluorescent biological labels, *Science* 281 (1998) 2013–2015.
- [13] B. Dubertret, Quantum dots: DNA detectives, *Nature Materials* 4 (2005) 797–798.
- [14] M. Hahn, P. Keng, T. Krauss, Flow cytometric analysis to detect pathogens in bacterial cell mixtures using semiconductor quantum dots, *Analytical Chemistry* 80 (2008) 864–872.
- [15] S. Wang, J. Wen, Y. Zhou, Z. Zhang, R. Yang, J. Zhang, J. Chen, X. Zhang, Identification and characterization of *Bacillus anthracis* by multiplex PCR on a DNA chip, *Biosensors and Bioelectronics* 20 (2004) 806–812.
- [16] G. Campbell, R. Mutharasan, Detection of *Bacillus anthracis* spores a model protein using PEMC sensors in a flow cell at 1 mL/min, *Biosensors and Bioelectronics* 22 (2006) 78–85.
- [17] A. Davila, J. Jang, A. Gupta, T. Walter, A. Aronson, R. Bashir, Microresonator mass sensors for detection of *Bacillus anthracis* Sterne spores in air water, *Biosensors and Bioelectronics* 22 (2007) 3028–3035.
- [18] T. Leighton, R. Doi, The stability of messenger ribonucleic acid during sporulation in *Bacillus subtilis*, *Journal of Biological Chemistry* 246 (1971) 3189–3195.
- [19] H. Kim, J. Goepfert, A sporulation medium for *Bacillus anthracis*, *Journal of Applied Bacteriology* 37 (1974) 265–267.
- [20] J. Ireland, P. Hanna, Amino-acid purine ribonucleoside-induced germination of *Bacillus anthracis* Δ Sterne endospores: *gerS* mediates responses to aromatic ring structures, *Journal of Bacteriology* 184 (2002) 1296–1303.
- [21] H. Tamir, C. Gilvarg, Density gradient centrifugation for the separation of sporulating forms of bacteria, *Journal of Biological Chemistry* 241 (1966) 1085–1090.
- [22] G. Hermanson, *Bioconjugate Techniques*, Academic Press, California, 1995.
- [23] D. Williams, O. Benedek, C. Turnbough Jr., Species-specific peptide ligands for the detection of *Bacillus anthracis* spores, *Applied and Environmental Microbiology* 69 (2003) 6288–6293.
- [24] T. Park, J. Park, G. Seo, Y. Chai, S. Lee, Rapid accurate detection of *Bacillus anthracis* spores using peptide-quantum dot conjugates, *Journal of Microbiology and Biotechnology* 16 (2006) 1713–1719.
- [25] W. Chang, T. Jiang, Z. Wan, J. Zhang, Z. Yang, D. Liang, Crystal structure of R-phycoerythrin from *Polysiphonia urceolata* at 2.8 Å resolution, *Journal of Molecular Biology* 262 (1996) 721–731.
- [26] J. Hesselgesser, M. Liang, J. Hoxie, M. Greenberg, L. Brass, M. Orsini, D. Taub, R. Horuk, Identification and characterization of the CXCR4 chemokine receptor in human T cell lines: ligand binding biological activity HIV-1 infectivity, *Journal of Immunology* 160 (1998) 877–883.
- [27] A. Barnaby, T. Dubrovsky, Quantum dots in flow cytometry, in: C. Hotz, M. Bruchez (Eds.), *Methods in Molecular Biology*, vol. 374, Humana Press, New York, 2007, pp. 185–203.
- [28] J. Boydston, L. Yue, J. Kearney, C. Turnbough Jr., The ExsY protein is required for complete formation of the exosporium of *Bacillus anthracis*, *Journal of Bacteriology* 188 (2006) 7440–7448.
- [29] C. Laflamme, D. Verreault, S. Lavigne, L. Trudel, J. Ho, C. Duchaine, Autofluorescence as a viability marker for detection of bacterial spores, *Frontiers in Bioscience* 10 (2005) 1647–1653.
- [30] J. Ness, R. Akhtar, C. Latham, K. Roth, Combined tyramide signal amplification and quantum dots for sensitive and photostable immunofluorescence detection, *The Journal of Histochemistry and Cytochemistry* 51 (2003) 981–987.
- [31] P. Gerhardt, E. Ribl, Ultrastructure of the exosporium enveloping spores of *Bacillus cereus*, *Journal of Bacteriology* 88 (1964) 1774–1789.
- [32] P. Sylvestre, E. Couture-Tosi, M. Mock, A collagen-like surface glycoprotein is a structural component of the *Bacillus anthracis* exosporium, *Molecular Microbiology* 45 (2002) 169–178.
- [33] J. Daubenspeck, H. Zeng, P. Chen, S. Dong, C. Steichen, N. Krishna, D. Pritchard, C. Turnbough Jr., Novel oligosaccharide side chains of the collagen-like region of BclA the major glycoprotein of the *Bacillus anthracis* exosporium, *The Journal of Biological Chemistry* 279 (2004) 30945–30953.
- [34] T. Brahmabhatt, B. Janes, E. Stibitz, S. Darnell, P. Sanz, S. Rasmussen, A. O'Brien, *Bacillus anthracis* exosporium protein BclA affects spore germination, interaction with extracellular matrix proteins, and hydrophobicity, *Infection and Immunity* 75 (2007) 5233–5239.
- [35] W. Schumacher, C. Storzuk, P. Dutta, A. Phipps, Identification and characterization of *Bacillus anthracis* spores by multiparameter flow cytometry, *Applied and Environmental Microbiology* 74 (2008) 5220–5223.
- [36] B. Ferrari, P. Bergquist, Quantum dots as alternatives to organic fluorophores for *Cryptosporidium* detection using conventional flow cytometry and specific monoclonal antibodies: lessons learned, *Cytometry Part A* 71 (2007) 265–271.
- [37] M. Smith, K. Thompson (Eds.), *Cryptosporidium*, The Analytical Challenge, Royal Society of Chemistry, London, 2001, pp. 1–162.
- [38] S. Dwarakanath, J. Bruno, A. Shastry, T. Phillips, A. John, A. Kumar, L. Stephensen, Quantum dot-antibody and aptamer conjugates shift fluorescence upon binding bacteria, *Biochemical and Biophysical Research Communications* 325 (2004) 739–743.